

# Asymptotic Analysis for the Mean First Passage Time in Finite or Spatially Periodic 2-D Domains with a Cluster of Small Traps

S. Iyaniwura<sup>1</sup>      M. J. Ward<sup>2</sup>

December 19, 2020

## Abstract

A hybrid asymptotic-numerical method is developed to approximate the mean first passage time and the splitting probability for a Brownian particle in a bounded 2-D domain that contains absorbing disks, referred to as “traps”, of asymptotically small radii. In contrast to previous studies that required traps to be spatially well-separated, we show how to readily incorporate the effect of a cluster of closely-spaced traps by adapting the least-squares approach of Trefethon [17] [ANZIAM J., **60**, (2018), pp. 1-26] in order to numerically solve certain local problems for the Laplacian near the cluster. We also provide new asymptotic formulae for the MFPT in 2-D spatially periodic domains where a trap cluster is centered at the lattice points of an oblique Bravais lattice. Over all such lattices with fixed area for the primitive cell, and for each specific trap set, the average MFPT is smallest for a hexagonal lattice of traps.

## Contents

<b>1</b>	<b>Introduction</b>	<b>2</b>
<b>2</b>	<b>Mean first passage time with a trap cluster</b>	<b>4</b>
2.1	Computing the logarithmic capacitance $d_{1c}$ . . . . .	5
2.2	Example: MFPT for a trap cluster in the unit disk . . . . .	7
<b>3</b>	<b>Splitting probability with a cluster of traps</b>	<b>10</b>
3.1	Example: The unit disk with a trap cluster . . . . .	13

1	<i>Introduction</i>	2
4	<b>Spatially periodic trap patterns</b>	<b>18</b>
4.1	The MFPT . . . . .	18
5	<b>Discussion</b>	<b>23</b>
A	<b>Dipole Moment: Two-Trap Cluster</b>	<b>24</b>

# 1 Introduction

Narrow capture problems are first passage time problems that predict the expected time it takes for a Brownian particle to become absorbed by a set of small measure. Narrow capture problems arise in various applications such as, determining the time it takes for a receptor to reach a specific small binding site, the time it takes for a diffusing surface-bound receptor to reach a small target site on the cell membrane, or the time it takes for a predator to locate its prey (cf. [1], [5], [8], [15], [12], [11]). An overview of applications of narrow capture and escape problems with biophysical applications is given in [7]. More recently, extended narrow capture problems involving stochastic search processes in finite domains with small traps have been analyzed in 3-D [3] and in 2-D [2].

In a 2-D bounded domain  $\Omega$ , a narrow capture problem is of singular perturbation type, characterized by the  $\mathcal{O}(1)$  spatial scale of the confining domain and an  $\mathcal{O}(\varepsilon) \ll 1$  scale for the multiply-connected absorbing set, which is modeled by a collection of absorbing non-overlapping disks of radii  $\mathcal{O}(\varepsilon)$ , referred to as “traps”. In the limit  $\varepsilon \rightarrow 0$  of small trap radius, strong localized perturbation theory, originating in [19] and [20] (see the survey [18]), was extended in [11] to derive linear algebraic systems that asymptotically predict the mean first passage time (MFPT) and the splitting probability for this 2-D narrow capture problem with an error smaller than any power of  $-1/\log \varepsilon$ . Here the splitting probability is defined as the probability for a Brownian particle, which starts from some point in the 2-D domain, to be captured by a specific target trap before becoming absorbed by any of the other traps in the domain. However, a key limitation of the analysis of [11] is that the disk-shaped traps were assumed to be well-separated in the sense that their center-to-center separation is  $\mathcal{O}(1)$  as  $\varepsilon \rightarrow 0$ . This restriction precluded studying the effect of a cluster of closely-spaced traps, such as shown schematically in Fig. 1.

One goal of this paper is to combine the recent simple series-based numerical method of [17] for Laplace’s equation on unbounded domains with the strong localized asymptotic framework of [11] in order to calculate the MFPT

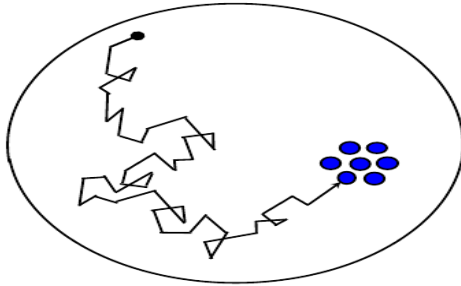


Figure 1: Schematic diagram of a Brownian particle in a disk that contains a hexagonal cluster of circular traps (blue disks) of a common radius  $\varepsilon$ .

and splitting probability when the 2-D confining domain contains a localized cluster of closely-spaced circular traps (see Fig. 1). The numerical approach of [17] is reformulated, as an alternative to a more involved and computationally intensive boundary integral numerical approach, to calculate solutions to two different “local” or inner problems involving Laplace’s equation on a locally unbounded domain that are needed in the linear algebraic systems of [11] so as to determine the asymptotic MFPT and splitting probability with an error smaller than any power of  $-1/\log \varepsilon$ . In particular, for the MFPT calculation in §2 we extend the approach in [17] to readily compute the logarithmic capacitance of the cluster of traps, as specified below by the constant term in the far-field behavior in (2.4) from the solution to Laplace’s equation defined locally near the trap cluster. The logarithmic capacitance is available analytically only for a few specific trap shapes (cf. [13]). For the splitting probability application in §3, we modify the approach of [17] so as to compute a harmonic measure and a dipole moment of the clustered trap set. We then extend the analytical theory of [11] for the splitting probability to one higher order so as to include the effect of the dipole of the clustered trap set. Our strategy of combining the strong localized perturbation approach in [11] with the simple numerical procedure of [17], which readily solves certain key local problems, is illustrated for a few specific narrow capture problems that have clear qualitative interpretations. Results from our hybrid asymptotic-numerical approach are favorably compared with corresponding results obtained from full PDE numerical simulations using FlexPDE [6].

The second goal of this paper, as undertaken in §4, is to use strong localized perturbation theory to provide new asymptotic formulae for the MFPT in a spatially periodic 2-D domain where a trap cluster is centered at the lattice points of an arbitrary oblique Bravais lattice. The average MFPT, accurate to all orders in  $\mathcal{O}(-1/\log \varepsilon)$ , is shown to depend on the regular part

of the source-neutral Green's function defined on the fundamental Wigner-Sietz cell for the lattice. An explicit formula for this regular part was derived previously in [4] in the study of the stability of small droplet patterns in the reaction-diffusion modeling of diblock copolymers. Our asymptotic result shows that, among all 2-D Bravais lattices with fixed area for the primitive cell, the average MFPT is smallest for a hexagonal arrangement of traps. For the special case of a square lattice our result for the average MFPT agrees with that in [16].

## 2 Mean first passage time with a trap cluster

The mean first passage time (MFPT) for a Brownian particle, with diffusivity  $D$ , that starts at a point  $\mathbf{x} \in \Omega \subset \mathbb{R}^2$  to be absorbed by a collection of trap in a domain with a reflecting boundary satisfies (cf. [14])

$$\begin{aligned} \Delta T &= -\frac{1}{D}, \quad \mathbf{x} \in \Omega \setminus \cup_{j=1}^N \Omega_j^\varepsilon, \quad \text{with} \quad \Omega_1^\varepsilon \equiv \cup_{i=1}^m \Omega_{1,i}^\varepsilon, \\ T &= 0, \quad \mathbf{x} \in \partial\Omega_j^\varepsilon, \quad j = 1, \dots, N; \quad \partial_n T = 0, \quad \mathbf{x} \in \partial\Omega. \end{aligned} \quad (2.1)$$

We will assume that the well-separated traps  $\Omega_j^\varepsilon$  for  $j = 2, \dots, N$  are disks of a common radius  $\varepsilon \ll 1$ . However, the possibly multiply-connected trap set  $\Omega_1^\varepsilon$ , centered at some  $\mathbf{x}_1 \in \Omega$ , is composed of  $m \geq 1$  non-overlapping disks  $\Omega_{1,i}^\varepsilon$  of a common radius  $\varepsilon \ll 1$ , for  $i = 1, \dots, m$ . Since the distance between  $\Omega_{1,i}^\varepsilon$  and  $\Omega_{1,k}^\varepsilon$  for  $i \neq k$  is assumed to be  $\mathcal{O}(\varepsilon)$ , we will refer to  $\Omega_1^\varepsilon$  as a *clustered trap set*. In the limit  $\varepsilon \rightarrow 0$ , strong localized perturbation theory, originating from [19] and surveyed in [18], can be used as in [11] to derive the following asymptotic approximation for  $T$ , and the average MFPT  $\bar{T}$  given by  $\bar{T} \sim |\Omega|^{-1} \int_\Omega T(\mathbf{x}) d\mathbf{x}$ :

**Principal Result 2.1:** *For  $\varepsilon \rightarrow 0$ , the asymptotic solution for the MFPT (2.1) in the outer region, defined by  $|\mathbf{x} - \mathbf{x}_j| \gg \mathcal{O}(\varepsilon)$  for  $j = 1, \dots, N$ , is*

$$T \sim -2\pi \sum_{j=1}^N A_j G(\mathbf{x}; \mathbf{x}_j) + \bar{T}, \quad (2.2a)$$

where  $A_j$ , for  $j = 1, \dots, N$ , and  $\bar{T}$  are the solution to the linear system

$$\frac{A_j}{\nu_j} + 2\pi R_j A_j + 2\pi \sum_{k \neq j}^N A_k G_{jk} = \bar{T}, \quad j = 1, \dots, N; \quad \sum_{k=1}^N A_k = \frac{|\Omega|}{2\pi D}, \quad (2.2b)$$

where  $R_j \equiv R(\mathbf{x}_j)$  and  $G_{jk} \equiv G(\mathbf{x}_j; \mathbf{x}_k)$ . Here  $\nu_j \equiv -1/\log \varepsilon$  for  $j = 2, \dots, N$  for the isolated circular traps, while  $\nu_1 \equiv -1/\log(\varepsilon d_{1c})$  for the clustered

trap set, with  $d_{1c}$  defined by the PDE (2.4). In (2.2),  $G(\mathbf{x}; \boldsymbol{\xi})$  is the unique Neumann Green's function for  $\Omega$  with regular part  $R(\boldsymbol{\xi})$  satisfying

$$\begin{aligned} \Delta G(\mathbf{x}; \boldsymbol{\xi}) &= \frac{1}{|\Omega|} - \delta(\mathbf{x} - \boldsymbol{\xi}), \quad \mathbf{x} \in \Omega; \quad \partial_n G = 0, \quad \mathbf{x} \in \partial\Omega, \\ G &\sim -\frac{1}{2\pi} \log |\mathbf{x} - \boldsymbol{\xi}| + R(\boldsymbol{\xi}) + o(1), \quad \text{as } \mathbf{x} \rightarrow \boldsymbol{\xi}; \quad \int_{\Omega} G d\mathbf{x} = 0. \end{aligned} \quad (2.3)$$

The central new feature for (2.2b) is that  $d_{1c}$  is the logarithmic capacitance for the clustered trap set  $\Omega_1^\varepsilon$ . It is defined by the following local problem, written in terms of the stretched coordinate  $\mathbf{y} = \varepsilon^{-1}(\mathbf{x} - \mathbf{x}_1)$  and subdomains  $\Omega_{1,i} \equiv \varepsilon^{-1}\Omega_{1,i}^\varepsilon$ , for  $i = 1, \dots, m$ , comprising the trap cluster:

$$\begin{aligned} \Delta_{\mathbf{y}} v_c &= 0, \quad \mathbf{y} \notin \cup_{i=1}^m \Omega_{1,i}; \quad v_c = 0, \quad \mathbf{y} \in \partial\Omega_{1,i}, \quad i = 1, \dots, m, \\ v_c &\sim \log |\mathbf{y}| - \log d_{1c} + \frac{\mathbf{p}_c \cdot \mathbf{y}}{|\mathbf{y}|^2} + \dots, \quad \text{as } |\mathbf{y}| \rightarrow \infty. \end{aligned} \quad (2.4)$$

Here  $\mathbf{p}_c$  is the dipole vector for the cluster. For this exterior problem in potential theory, the key quantity to be determined in the MFPT analysis is  $d_{1c}$ , representing the logarithmic capacitance of the cluster. In general,  $d_{1c}$  must be computed numerically. In Fig. 2 we show the local geometry associated with (2.4) for a two-trap cluster with  $m = 2$  (left panel) and for a hexagonal trap cluster with  $m = 7$  (right panel).



Figure 2: Left panel: two circular traps each of unit radius in the inner region with center-to-center separation  $l_c$ . Right panel: a hexagonal arrangement of traps with a center trap at a distance  $l_c$ .

## 2.1 Computing the logarithmic capacitance $d_{1c}$

Although in general  $d_{1c}$  must be computed numerically from (2.4), it can be determined analytically for the special case where two disks, each of radius

one (measured in the inner coordinate), have a center-to-center separation  $l_c$ , such as shown in the left panel of Fig. 2. For this geometry, (2.4) can be solved analytically using bipolar coordinates. This leads to the following explicit result for  $d_{1c}$  (see Appendix A of [11]):

$$\log d_{1c} = \frac{1}{2} \log (l_c^2 - 4) - \frac{\beta}{2} + \sum_{k=1}^{\infty} \frac{e^{-k\beta}}{k \cosh(k\beta)}, \quad \beta \equiv \cosh^{-1} (l_c/2). \quad (2.5)$$

We now show how to reformulate the simple numerical approach introduced in [17], based on a series solution to Laplace's equation coupled to a least squares fitting of the boundary condition in (2.4), in order to numerically compute  $d_{1c}$  for a cluster of disks. We will illustrate our approach for the hexagonal array of traps shown in the right panel of Fig. 2. By reformulating the series-based method of [17], we obtain from equations (3.1) and (3.2) of [17] that  $v_c$  must have the form

$$v_c(z) = -\log d_{1c} + \sum_{j=1}^m e_j \log |z - c_j| + \sum_{j=1}^m \sum_{k=1}^n \left( a_{jk} \operatorname{Re}(z - c_j)^{-k} + b_{jk} \operatorname{Im}(z - c_j)^{-k} \right), \quad (2.6)$$

together with the condition that  $\sum_{j=1}^m e_j = 1$ . Here,  $z \in \mathbb{C}$  is equivalent to the point  $\mathbf{y}$  in complex coordinates,  $c_j \in \mathbb{C}$  is the center of the  $j^{\text{th}}$  trap in the cluster, and  $m$  is the number of traps in the cluster. The real-valued constants  $\log d_{1c}$ ,  $e_j$ ,  $a_{jk}$ , and  $b_{jk}$  for  $j = 1, \dots, m$  and  $k = 1, \dots, n$  are determined such that  $v_c = 0$  is satisfied in the least-squares sense on the boundary of each trap. By using the fact that  $\log |z - c_j| \simeq \log |z| - o(1)$  as  $|z| \rightarrow \infty$ , it can easily be verified that (2.6) satisfies the far-field behavior of  $v_c$  as  $|\mathbf{y}| \rightarrow \infty$  specified in (2.4). To fit the boundary condition on each trap, we impose that  $v_c(z) = 0$  at  $3n$  uniformly spaced points on the boundary of each trap. This leads to a  $3nm + 1$  dimensional algebraic system of equations with  $(2nm + m + 1)$  unknowns. This system was then solved in the least-squares sense using the backslash command in MATLAB. Choosing  $n = 10$ , for the two-trap cluster (left panel of Fig. 2), this corresponds to 61 algebraic equations with 43 unknowns, while for the hexagonal cluster (right panel of Fig. 2), we have 211 equations and 148 unknowns.

For the two-trap cluster, in the left panel of Fig. 3 we show that the numerical result for  $d_{1c}$  from the least-squares fit (2.6) compares very favorably with the analytical result (2.5). In the right panel of Fig. 3 we plot the absolute value of the error obtained in approximating the exact result (2.5) for

$d_{1c}$  with the least squares fit based on (2.6) with  $n = 5$  and  $n = 10$  terms. We observe that the accuracy of the fit improves as the separation between the disks increases and that  $n = 10$  terms gives a very accurate result. In the left panel of Fig. 3 we also plot  $d_{1c}$  versus  $l_c$  for the hexagonal trap cluster, as computed from the least-squares fit on (2.6). For a hexagonal trap cluster an analytical solution of (2.4) is not available.

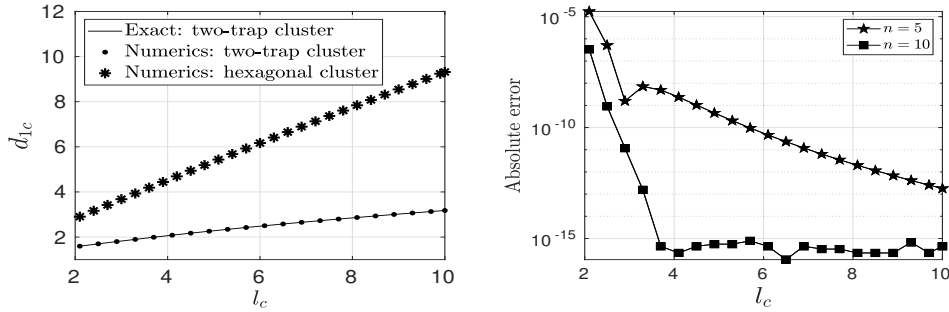


Figure 3: Left panel: Logarithmic capacitance  $d_{1c}$  versus the inter-trap separation  $l_c > 2$  (see Fig. 2) for a two-trap cluster from the explicit formula (2.5) (solid line) and the least squares result of (2.6) (round points). The corresponding least squares result of (2.6) for the hexagonal cluster are the starred points. As  $l_c \rightarrow 2^+$  the disks begin to touch. Right panel: Absolute error between the exact formula for  $d_{1c}$  in (2.5) for a two-disk cluster and the numerical result computed using (2.6) and the least squares fit with  $n = 5$  and  $n = 10$  terms. Observe that  $n = 10$  provides a highly accurate result.

## 2.2 Example: MFPT for a trap cluster in the unit disk

To illustrate (2.2) and the effect of a clustered trap set, we let  $\Omega$  be the unit disk and assume that  $N = 1$ , so that the only traps in  $\Omega$  are within a trap cluster centered at  $\mathbf{x}_1 \in \Omega$ . From (2.2), the average MFPT is

$$\bar{T} \equiv \bar{T}(\varepsilon) \sim \frac{|\Omega|}{2\pi D} \left( \frac{1}{\nu_1} + 2\pi R(\mathbf{x}_1) \right), \quad \nu_1 = -1/\log(\varepsilon d_{1c}), \quad (2.7a)$$

where  $|\Omega| = \pi$ . For the unit disk, the Neumann Green's function and its regular part are (see equation (4.3) of [10])

$$G(\mathbf{x}; \mathbf{x}_1) = -\frac{1}{2\pi} \log |\mathbf{x} - \mathbf{x}_1| - \frac{1}{4\pi} \log (|\mathbf{x}|^2 |\mathbf{x}_1|^2 + 1 - 2\mathbf{x} \cdot \mathbf{x}_1) + \frac{(|\mathbf{x}|^2 + |\mathbf{x}_1|^2)}{4\pi} - \frac{3}{8\pi}, \quad (2.7b)$$

$$R(\mathbf{x}_1) = -\frac{1}{2\pi} \log(1 - |\mathbf{x}_1|^2) + \frac{|\mathbf{x}_1|^2}{2\pi} - \frac{3}{8\pi}. \quad (2.7c)$$

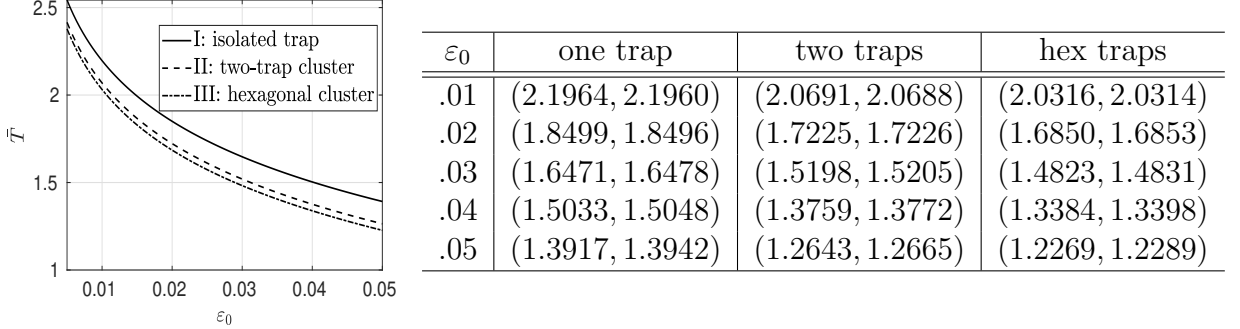


Figure 4: Left panel: Average MFPT  $\bar{T}$  in (2.7) for a trap cluster centered at  $(0.5, 0)^T$  in the unit disk. Case I: single isolated trap of radius  $\varepsilon_0$ . Case II: a two-trap cluster with traps of radius  $\varepsilon_0/\sqrt{2}$  with center-to-center separation  $\varepsilon_0 l_c/\sqrt{2}$  with  $l_c = 3$ . Case III: a hexagonal cluster with traps of radius  $\varepsilon_0/\sqrt{7}$  with separation  $\varepsilon_0 l_c/\sqrt{7}$  with  $l_c = 3$ . In each case, the traps occupy the same area  $\pi\varepsilon_0^2$ . Right panel: A comparison of the asymptotic result  $\bar{T}$  with the FlexPDE numerical result  $\bar{T}_n$  at a few  $\varepsilon_0$  in the form  $(\bar{T}, \bar{T}_n)$ .

To show the effect of the trap set, we compare (2.7) for three scenarios when  $\mathbf{x}_1 = (0.5, 0)^T$  and  $D = 1$ , and where we have fixed the total area of the trap set at  $\pi\varepsilon_0^2$ . Case I: a single isolated trap of radius  $\varepsilon_0$ , for which  $d_{1c} = 1$ . Case II: a two-trap cluster with traps of radius  $\varepsilon_0/\sqrt{2}$  and center-to-center separation  $\varepsilon_0 l_c/\sqrt{2}$  with  $l_c = 3$ , for which  $d_{1c} \approx 1.8245$  from (2.5). Case III: a hexagonal trap cluster with traps of radius  $\varepsilon_0/\sqrt{7}$  and center-to-center separation  $\varepsilon_0 l_c/\sqrt{7}$  with  $l_c = 3$ , for which  $d_{1c} \approx 3.6791$  from (2.6). In the left panel of Fig. 4 we compare the asymptotic results  $\bar{T}(\varepsilon_0)$ ,  $\bar{T}(\varepsilon_0/\sqrt{2})$ , and  $\bar{T}(\varepsilon_0/\sqrt{7})$  for these three scenarios, where  $\bar{T}(\varepsilon)$  is defined in (2.7). From this figure, we observe as expected that the MFPT is smallest for the hexagonal trap cluster. As a qualitative explanation of this result, we note that for the hexagonal trap cluster the absorbing traps have a combined perimeter of  $7(2\pi\varepsilon_0/\sqrt{7}) = \sqrt{7}\pi\varepsilon_0$ , which is larger than that for the two-trap cluster or for the single trap. With a larger trap perimeter it should be easier to capture a Brownian particle. However, as the number of traps in a cluster increases, there should be less of a marginal decrease in the MFPT owing to the presence of shielded traps, not on the periphery of cluster, that are unlikely to be reached by a Brownian particle wandering in  $\Omega$ . In the right panel of Fig. 4 we show a very favorable comparison between the asymptotic results for  $\bar{T}$  and the corresponding full PDE results computed from (2.1)

using FlexPDE [6]. In Fig. 5 we show a contour plot of the FlexPDE result for  $T$  for a two-trap and a hexagonal trap cluster. For a two-trap cluster, in Fig. 6 we show a contour plot of the asymptotic result in (2.2a) of Principal Result 2.1 for the outer solution, which is for the same parameters used for the FlexPDE results shown in the left panel of Fig. 5. The asymptotic and FlexPDE results are nearly indistinguishable.

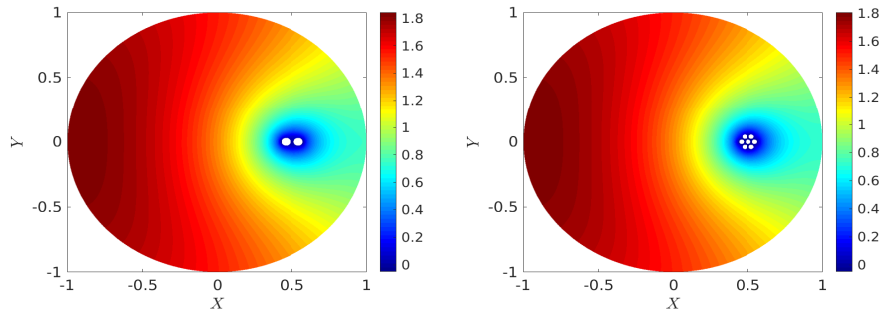


Figure 5: Contour plots of  $T$  from FlexPDE [6] for a two-trap cluster (left) and a hexagonal cluster (right) with  $\varepsilon_0 = 0.04$ ,  $l_c = 3$ , and  $D = 1$ . Left: traps have radii  $\varepsilon_0/\sqrt{2}$  and center-to-center separation  $l_c\varepsilon_0/\sqrt{2}$ . Right: traps have radii  $\varepsilon_0/\sqrt{7}$  and center-to-center separation  $l_c\varepsilon_0/\sqrt{7}$ .

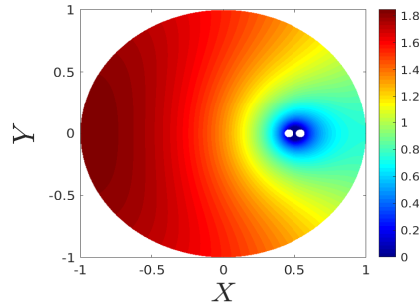


Figure 6: Contour plot of  $T$  in the outer region from the asymptotic theory (2.2a) of Principal Result 2.1 for a two-trap cluster with parameters  $D = 1$ ,  $l_c = 3$ ,  $\varepsilon_0 = 0.04$ . The traps have radii  $\varepsilon_0/\sqrt{2}$  and center-to-center separation  $l_c\varepsilon_0/\sqrt{2}$ . The asymptotic results agree closely with the FlexPDE result in the left panel of Fig. 5.

### 3 Splitting probability with a cluster of traps

In this section we develop a similar approach as done for the MFPT to calculate the splitting probability for a collection of  $N$  traps that consists of  $N - 1$  isolated traps together with a trap cluster. Our goal is to calculate the splitting probability, defined as the probability of reaching a particular trap located within the trap cluster, before reaching any of the other possible traps. We will assume that all traps are non-overlapping disks of a common radius  $\varepsilon$ . The closely spaced traps within a cluster of size  $\mathcal{O}(\varepsilon)$  are centered at some  $\mathbf{x}_1 \in \Omega$ , while the  $N - 1$  isolated traps are centered at  $\mathbf{x}_j \in \Omega$  for  $j = 2, \dots, N$ . For this configuration of traps, the splitting probability  $P(\mathbf{x})$  satisfies (cf. [14])

$$\begin{aligned} \Delta P &= 0, \quad \mathbf{x} \in \Omega \setminus \cup_{j=1}^N \Omega_j^\varepsilon, \quad \Omega_1^\varepsilon \equiv \cup_{i=1}^m \Omega_{1,i}^\varepsilon; \quad \partial_n P = 0, \quad \mathbf{x} \in \partial\Omega, \\ P &= 0, \quad \mathbf{x} \in \partial\Omega_j^\varepsilon, \quad j = 2, \dots, N, \\ P &= 1, \quad \mathbf{x} \in \partial\Omega_{1,1}^\varepsilon; \quad P = 0, \quad \mathbf{x} \in \partial\Omega_{1,i}^\varepsilon, \quad i = 2, \dots, m, \end{aligned} \quad (3.1)$$

where the target trap within the cluster is labeled by  $\Omega_{1,1}^\varepsilon$ .

To analyze (3.1) we must consider a new inner problem near the multi-trap cluster  $\Omega_1^\varepsilon$ . In this inner region, we introduce local variables  $\mathbf{y} = \varepsilon^{-1}(\mathbf{x} - \mathbf{x}_1)$  and  $v(\mathbf{y}) = P(\mathbf{x}_1 + \varepsilon\mathbf{y})$ , and we decompose  $v$  as

$$v \sim v^* + A_1 v_c, \quad (3.2)$$

where  $A_1$  is a constant to be found and  $v_c$  satisfies (2.4), which determines the logarithmic capacitance  $d_{1c}$  of the cluster. In (3.2), the bounded function  $v^*(\mathbf{y})$ , with limiting value  $v_\infty^*$  to be determined, is taken to satisfy

$$\begin{aligned} \Delta_{\mathbf{y}} v^* &= 0, \quad \mathbf{y} \notin \cup_{k=1}^m \Omega_{1,k}; \quad v^* \sim v_\infty^* + \frac{\mathbf{p}_\infty \cdot \mathbf{y}}{|\mathbf{y}|^2} + \dots, \quad \text{as } |\mathbf{y}| \rightarrow \infty, \\ v^* &= 1, \quad \mathbf{y} \in \partial\Omega_{1,1}; \quad v^* = 0, \quad \mathbf{y} \in \partial\Omega_{1,k}, \quad k = 2, \dots, m, \end{aligned} \quad (3.3)$$

where  $\Omega_{1,k} \equiv \varepsilon^{-1}\Omega_{1,k}^\varepsilon$  for  $k = 1, \dots, m$ .

In terms of the inner problem (3.3), the asymptotic result for (3.1), as derived in §5 of [11], and extended here to include the  $\mathcal{O}(\varepsilon)$  correction term arising from the dipole moment of the trap cluster, is as follows:

**Principal Result 3.1:** *For  $\varepsilon \rightarrow 0$ , the asymptotic solution for the splitting probability in the outer region  $|\mathbf{x} - \mathbf{x}_j| \gg \mathcal{O}(\varepsilon)$  for  $j = 1, \dots, N$  is*

$$P \sim -2\pi \sum_{j=1}^N A_j G(\mathbf{x}; \mathbf{x}_j) + \chi + 2\pi\varepsilon [\mathbf{p}_\infty + A_1 \mathbf{p}_c] \cdot \nabla_{\mathbf{x}_1} G(\mathbf{x}; \mathbf{x}_1) + o(\varepsilon). \quad (3.4a)$$

Here  $\mathbf{p}_c$  and  $\mathbf{p}_\infty$  are the dipole vectors defined by the local problems (2.4) and (3.3), respectively. The constants  $A_j$  for  $j = 1, \dots, N$  and  $\chi$  are the solution to the linear system

$$\begin{aligned} \frac{A_j}{\nu_j} + 2\pi A_j R_j + \sum_{k \neq j}^N 2\pi A_k G_{jk} - \chi &= -\delta_{1,j} v_\infty^*, \quad j = 1, \dots, N, \\ \sum_{j=1}^N A_j &= 0, \end{aligned} \quad (3.4b)$$

where  $R_j \equiv R(\mathbf{x}_j)$ ,  $G_{jk} \equiv G(\mathbf{x}_j; \mathbf{x}_k)$  and  $\delta_{1,j}$  is the Kronecker symbol. Here  $\nu_j \equiv -1/\log \varepsilon$  for  $j = 2, \dots, N$  for the isolated circular traps, while  $\nu_1 \equiv -1/\log(\varepsilon d_{1c})$  for the trap cluster, with  $d_{1c}$  defined by (2.4). In (3.4),  $G$  is the Neumann Green's function with regular part  $R$  satisfying (2.3).

The  $\mathcal{O}(\varepsilon)$  term in (3.4a) is a new result that arises from the dipole term associated with the trap cluster. To derive this term we obtain that the far-field behavior of (3.2), when written in terms of the outer variable  $\mathbf{x}$ , yields the following matching condition for the outer solution:

$$P \sim v_\infty^* + A_1 \log |\mathbf{x} - \mathbf{x}_1| + \frac{A_1}{\nu_1} + \varepsilon \frac{(\mathbf{p}_\infty + A_1 \mathbf{p}_c) \cdot (\mathbf{x} - \mathbf{x}_1)}{|\mathbf{x} - \mathbf{x}_1|^2}, \quad \text{as } \mathbf{x} \rightarrow \mathbf{x}_1. \quad (3.5)$$

This enforces that in the outer region we expand  $P = P_0 + \varepsilon P_1 + \dots$ , and obtain that the correction  $P_1$  satisfies

$$\begin{aligned} \Delta P_1 &= 0, \quad \mathbf{x} \in \Omega \setminus \{\mathbf{x}_1\}; \quad \partial_n P_1 = 0, \quad \mathbf{x} \in \partial\Omega; \\ P_1 &\sim \frac{(\mathbf{p}_\infty + A_1 \mathbf{p}_c) \cdot (\mathbf{x} - \mathbf{x}_1)}{|\mathbf{x} - \mathbf{x}_1|^2}, \quad \text{as } \mathbf{x} \rightarrow \mathbf{x}_1. \end{aligned} \quad (3.6)$$

We remark that since the other well-separated traps for  $j = 2, \dots, N$  are disks, there is no dipole term arising at  $\mathcal{O}(\varepsilon)$  from these other traps. The problem (3.6) is equivalent to  $\Delta P_1 = -2\pi (\mathbf{p}_\infty + A_1 \mathbf{p}_c) \cdot \nabla_{\mathbf{x}_1} \delta(\mathbf{x} - \mathbf{x}_1)$ , where  $\delta(\mathbf{x} - \mathbf{x}_1)$  is the Dirac distribution. Since  $\Delta [\mathbf{a} \cdot \nabla_{\mathbf{x}_1} G(\mathbf{x}; \mathbf{x}_1)] = -\mathbf{a} \cdot \nabla_{\mathbf{x}_1} \delta(\mathbf{x} - \mathbf{x}_1)$  in  $\Omega$ , together with  $\partial_n [\mathbf{a} \cdot \nabla_{\mathbf{x}_1} G_p] = 0$  on  $\partial\Omega$ , holds for any constant vector  $\mathbf{a}$ , by choosing  $\mathbf{a} \equiv \mathbf{p}_\infty + A_1 \mathbf{p}_c$  we readily identify that the solution to (3.6) is given by the  $\mathcal{O}(\varepsilon)$  term in (3.4a).

In order to illustrate the asymptotic theory that leads to (3.4), we need a simple approach for calculating  $v_\infty^*$  and the dipole vector  $\mathbf{p}_\infty$  from (3.3). Following the approach of [17] used for the inner problem (2.4), we deduce

that  $v^*$  has the form

$$v^*(z) = v_\infty^* + \sum_{j=1}^m e_j \log |z - c_j| + \sum_{j=1}^m \sum_{k=1}^n \left( a_{jk} \operatorname{Re}(z - c_j)^{-k} + b_{jk} \operatorname{Im}(z - c_j)^{-k} \right), \quad (3.7)$$

together with the condition that  $\sum_{j=1}^m e_j = 0$  so that the solution is bounded as  $|z| \rightarrow \infty$  and satisfies  $v^*(z) \rightarrow v_\infty^*$  as  $|z| \rightarrow \infty$ . In this formulation,  $z \in \mathbb{C}$  is equivalent to the point  $\mathbf{y}$  in complex coordinates,  $c_j \in \mathbb{C}$  is the center of the  $j^{\text{th}}$  trap, and  $m$  is the number of traps in the cluster. The real-valued constants  $v_\infty^*$ ,  $e_j$ ,  $a_{jk}$ , and  $b_{jk}$  for  $j = 1, \dots, m$  and  $k = 1, \dots, n$  are determined such that the boundary conditions in (3.3) are satisfied in the least squares sense. Following the same approach described above in §2.1 for implementing the boundary conditions, we obtain  $3nm + 1$  algebraic equations and  $2nm + m + 1$  unknowns. Choosing  $n = 10$ , this gives 211 algebraic equations and 148 unknowns for the hexagonal trap cluster, and 61 equations and 43 unknowns for the two-trap cluster.

Next, we let  $|z| \rightarrow \infty$  in (3.7) so as to identify the numerical approximation to the dipole term in the far-field behavior of (3.3). For  $|z| \gg 1$ , we use a Taylor approximation to estimate

$$\begin{aligned} \operatorname{Re}(z - c_j)^{-1} &\sim \frac{\operatorname{Re}(z)}{|z|^2}, & \operatorname{Im}(z - c_j)^{-1} &\sim \frac{\operatorname{Im}(\bar{z})}{|z|^2}, \\ \log |z - c_j| &\sim \log |z| - \frac{\operatorname{Re}(z\bar{c}_j)}{|z|^2} + \mathcal{O}(|z|^{-2}). \end{aligned} \quad (3.8)$$

Substituting these expressions into (3.7), and using  $\sum_{j=1}^m e_j = 0$ , we obtain for  $|z| \gg 1$ , with  $z = y_1 + iy_2$ , that

$$\begin{aligned} v_c &\sim v_\infty^* + \frac{y_1}{y_1^2 + y_2^2} \left( \sum_{j=1}^m (a_{j1} - e_j \operatorname{Re}(\bar{c}_j)) \right) \\ &\quad + \frac{y_2}{y_1^2 + y_2^2} \left( - \sum_{j=1}^m (b_{j1} - e_j \operatorname{Im}(\bar{c}_j)) \right) + \mathcal{O}(|\mathbf{y}|^{-2}). \end{aligned} \quad (3.9)$$

In this way, we identify that the approximation to the dipole vector  $\mathbf{p}_\infty$  in (3.3) is

$$\mathbf{p}_\infty \approx \left( \sum_{j=1}^m (a_{j1} - e_j \operatorname{Re}(\bar{c}_j)), - \sum_{j=1}^m (b_{j1} - e_j \operatorname{Im}(\bar{c}_j)) \right). \quad (3.10)$$

For a two-disk cluster with the target trap at  $\Omega_{1,1} = \{\mathbf{y} \mid |\mathbf{y} - \mathbf{y}_1| \leq 1\}$ , where  $\mathbf{y}_1 = (l_c/2, 0)^T$  and the other trap at  $\Omega_{1,2} = \{\mathbf{y} \mid |\mathbf{y} - \mathbf{y}_2| \leq 1\}$ , with  $\mathbf{y}_2 = (-l_c/2, 0)^T$ , we can calculate the dipole vector  $\mathbf{p}_\infty$  in (3.3) analytically for any  $l_c > 2$ . In Appendix A we derive that

$$\mathbf{p}_\infty = \left( \frac{\sqrt{(l_c/2)^2 - 1}}{\cosh^{-1}(l_c/2)}, 0 \right)^T. \quad (3.11)$$

In Fig. 7 we show a very favorable comparison between the analytical result (3.11) and the numerical result (3.10) based on the least-squares fit.

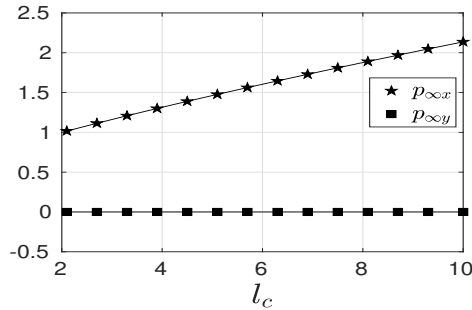


Figure 7: Comparison of the analytical result (3.11) (solid curve) with the numerical result (3.10) for the components of the dipole vector  $\mathbf{p}_\infty = (p_{\infty x}, p_{\infty y})^T$  for a two-trap cluster with center-to-center separation  $l_c$ .

### 3.1 Example: The unit disk with a trap cluster

We now illustrate (3.4b) when  $\Omega$  is the unit disk for the case  $N = 1$ , where the only traps in  $\Omega$  are within a clustered trap set. We find from (3.4b) that  $A_1 = 0$  and  $\chi = v_\infty^*$ , and so from (3.4a) and (2.7b) a two-term approximation for the splitting probability in the outer region is given by

$$P \sim v_\infty^* + 2\pi\varepsilon \mathbf{p}_\infty \cdot \nabla_{\mathbf{x}_1} G(\mathbf{x}; \mathbf{x}_1) + o(\varepsilon),$$

where

$$\nabla_{\mathbf{x}_1} G(\mathbf{x}; \mathbf{x}_1) = \frac{1}{2\pi} \left( \frac{\mathbf{x} - \mathbf{x}_1}{|\mathbf{x} - \mathbf{x}_1|^2} + \mathbf{x}_1 - \frac{|\mathbf{x}|^2 \mathbf{x}_1 - \mathbf{x}}{|\mathbf{x}|^2 |\mathbf{x}_1|^2 + 1 - 2\mathbf{x}_1 \cdot \mathbf{x}} \right). \quad (3.12)$$

For a two-trap cluster with identical traps, the far-field behavior of the solution to (3.3) gives  $v_\infty^* = 1/2$ , as can be readily proved by symmetry or by using bipolar coordinates (see [11]). Qualitatively, this leading order approximation for  $P$  shows that for any starting point  $\mathbf{x} \in \Omega$ , which is not within

an  $\mathcal{O}(\varepsilon)$  neighborhood of  $\mathbf{x}_1$ , it is to equally likely to first reach either of the two identical traps in the two-trap cluster. With this simple exact solution, as a check on the accuracy of the least-squares fit we obtained numerically that  $|v_\infty^* - 1/2| \leq 10^{-10}$  using  $n = 10$  in (3.7). However, the  $\mathcal{O}(\varepsilon)$  gradient term in (3.12) shows that the outer solution has a weak dependence on the orientation of the traps within the cluster.

$\varepsilon$	$P: \mathbf{x} = (-0.5, 0)^T$	$P: \mathbf{x} = (0.5, 0)^T$
.005	(0.48548, 0.48543)	(0.51452, 0.51451)
.01	(0.47096, 0.47088)	(0.52904, 0.52903)
.02	(0.44192, 0.44188)	(0.55808, 0.55804)
.03	(0.41287, 0.41308)	(0.58713, 0.58702)
.05	(0.35470, 0.35602)	(0.64521, 0.64397)

Figure 8: Comparison of the two-term result (3.12), labeled as  $P_a$  with the full PDE result  $P_n$  in the form  $(P_a, P_n)$  for a two-trap cluster centered at the origin with traps at  $\mathbf{x} = (-\varepsilon l_c/2, 0)^T$  and  $\mathbf{x} = (\varepsilon l_c/2, 0)^T$  with  $l_c = 3$ . The rightmost trap is the target trap where  $P = 1$ . The comparison at a few values of  $\varepsilon$  is done at the points  $\mathbf{x} = (\pm 0.5, 0)$  in the outer region.

To illustrate (3.12) we consider a two-disk cluster centered at the origin  $\mathbf{x}_1 = \mathbf{0}$  of the unit disk with traps centered at  $(\pm \varepsilon l_c/2, 0)^T$  in which  $P = 1$  and  $P = 0$  on the rightmost and leftmost traps, respectively. For this configuration, the dipole vector  $\mathbf{p}_\infty$  is given in (3.11). Fixing  $l_c = 3$ , in Table 8 we show a very favorable comparison for various  $\varepsilon$  between the two-term asymptotic result (3.12) and the corresponding full numerical results computed from the PDE (3.1) using FlexPDE [6] at the sample points  $\mathbf{x}_\pm = (\pm 0.5, 0)^T$ . From this table, we observe that the dipole term induces an asymmetry in the splitting probability on either side of the cluster. Upstream of the cluster at  $\mathbf{x}_+ = (0.5, 0)^T$  the target trap centered at  $(\varepsilon l_c/2, 0)^T$  is not shielded by the other trap in the cluster, and consequently  $P > 1/2$  at  $\mathbf{x} = \mathbf{x}_+$ . At this upstream point we observe very close agreement between the two-term asymptotic result (3.12) and the full PDE results. In addition, as a result of a shielding effect, we observe that  $P < 1/2$  at the downstream starting point  $\mathbf{x}_- = (-0.5, 0)^T$ . In the left panel of Fig. 9 we provide a contour plot of  $P$ , as computed from (3.1) using FlexPDE [6], which shows the effect of the dipole vector in the outer region. The corresponding plot of the asymptotic solution (3.12) in the outer region is shown in the right panel of Fig. 9 to very closely approximate the FlexPDE result.

Next, we consider the hexagonal clustered trap set in Fig. 2. By using (3.7) to approximate the solution to (3.3), in the left panel of Fig. 10 we

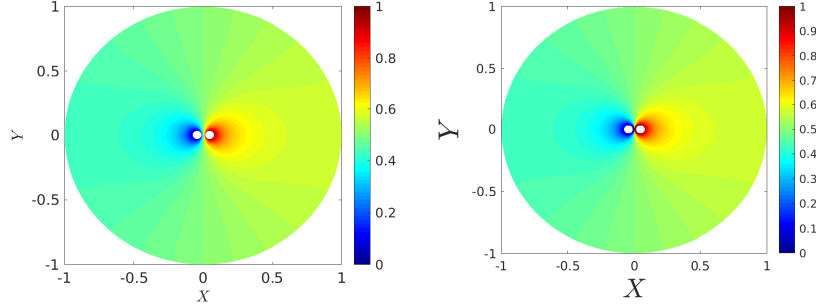


Figure 9: Left panel: Contour plot of the splitting probability  $P$  computed from the PDE (3.1) using FlexPDE [6] for a two-trap cluster centered at the origin in the unit disk with traps at  $\mathbf{x} = (-\varepsilon l_c/2, 0)^T$  and  $\mathbf{x} = (\varepsilon l_c/2, 0)^T$  with  $l_c = 3$  and  $\varepsilon = 0.03$ . The rightmost trap in the cluster is the target trap. The effect of the dipole term from the trap cluster is evident. Right panel: contour plot of the splitting probability in the outer region, as given in (3.12), from the asymptotic theory. The results are nearly indistinguishable.

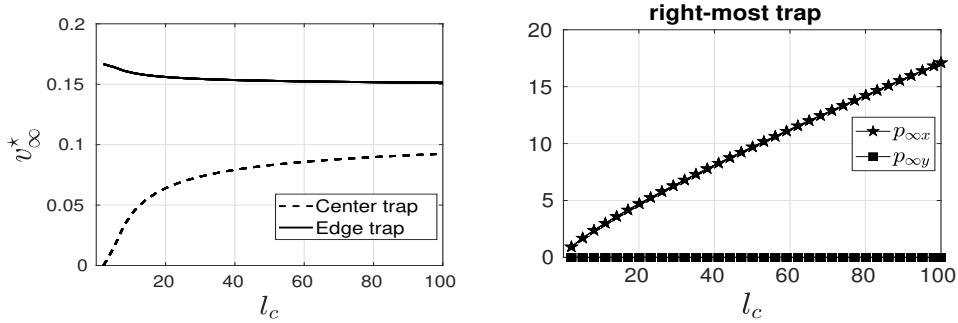


Figure 10: Left panel: Numerical result for  $v_\infty^*$ , defined by (3.3), and computed from a least-squares fit of (3.7), when either the target trap is on the edge (solid line) or at the center (dashed line) of the hexagonal cluster. Right panel: numerical result from (3.10) for the components of the dipole vector  $\mathbf{p}_\infty = (p_{\infty x}, p_{\infty y})^T$  for the hexagonal trap cluster with separation  $l_c$  and where the target trap is at the rightmost edge of the cluster.

plot the leading-order outer solution  $P \sim v_\infty^*$  versus  $l_c$  for the case where the target trap is either on the rightmost edge of the cluster (solid curve) or is at the center of the cluster (dashed curve). When  $l_c$  is only slightly above  $l_c = 2$ , corresponding to when the traps are closely packed, we observe as expected from Fig. 10 that  $P \sim v_\infty^* \approx 1/6$  when the target trap is at the edge of the cluster and that  $P$  is near zero when the target trap is shielded at the center of the cluster. As  $l_c$  increases, and the cluster becomes less packed, the shielding effect on the center trap decreases and it becomes increasingly likely to hit this trap first before any of the six traps on the periphery of the cluster. In the right panel of Fig. 10 we plot the components of the dipole vector  $\mathbf{p}_\infty = (p_{\infty x}, p_{\infty y})^T$  versus  $l_c$ , as computed numerically from (3.10), when the target trap is at the rightmost edge of the cluster. As a check on the numerics, we compute from (3.10) that  $|\mathbf{p}_\infty| \approx 10^{-16}$  when the target trap is at the center of the cluster. For this case, by symmetry we must have  $\mathbf{p}_\infty = (0, 0)^T$ .

As a further illustration of (3.12) we consider the hexagonal trap cluster centered at the origin  $\mathbf{x}_1 = \mathbf{0}$  of the unit disk with  $l_c = 3$ . We consider two scenarios. Case I: target trap, for which  $P = 1$ , is located at the center of the cluster. For this case, we have  $\mathbf{p}_\infty = (0, 0)^T$  and  $v_\infty^* \approx 8.745 \times 10^{-4}$  (dotted curve in the left panel of Fig. 10). Case II: target trap with  $P = 1$  is located at the rightmost trap of the cluster. For this case, we calculate  $v_\infty^* \approx 0.1665$  (solid curve in the left panel of Fig. 10) and  $\mathbf{p}_\infty \approx (1.1702, 0)^T$  from the right panel of Fig. 10.

For Case I, in Fig. 11 we show a favorable comparison at  $\mathbf{x} = (\pm 0.5, 0)^T$  between the spatially uniform asymptotic result  $P \sim v_\infty^* + o(\varepsilon)$  and the FlexPDE numerical result computed from the PDE (3.1). From this figure we observe no dipole effect and that the probability of reaching the target trap at the center of the hexagon before encountering any of the shielding traps on the periphery of the cluster is uniformly small when  $|\mathbf{x}| \gg \mathcal{O}(\varepsilon)$ .

Next, for Case II where the target trap is at the rightmost edge of the cluster, in the right panel of Fig. 12 we show that the two-term asymptotic (3.12) with  $v_\infty^* \approx 0.1665$  and dipole vector  $\mathbf{p}_\infty \approx (1.1702, 0)^T$  compares very favorably at  $\mathbf{x} = (\pm 0.5, 0)$  with the corresponding FlexPDE numerical result up to roughly  $\varepsilon \approx 0.03$ . The effect of the dipole term is evident in the FlexPDE contour plot shown in the left panel of Fig. 12. We observe that the effect of the dipole is to increase significantly the probability of first encountering the target trap starting from the upstream point  $(0.5, 0)^T$  in comparison to starting from the downstream location  $(-0.5, 0)^T$ .

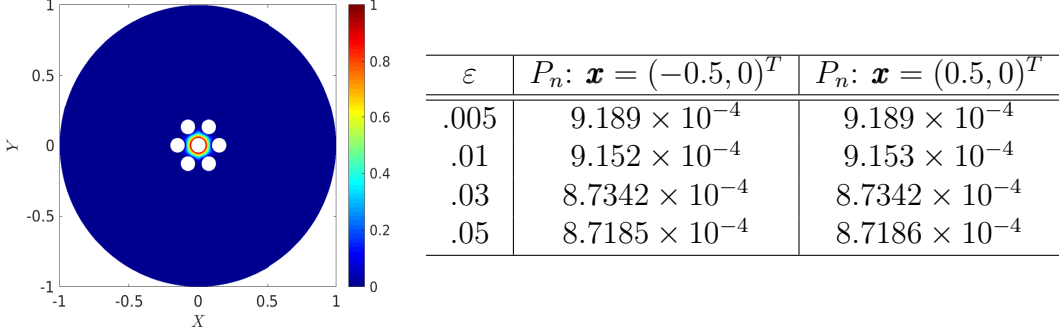


Figure 11: Right panel: The FlexPDE [6] numerical result  $P_n$  computed at  $(\pm 0.5, 0)^T$  for a hexagonal trap cluster centered at the origin of the unit disk with  $l_c = 3$ . The target trap with  $P = 1$  is at the center of the cluster and the dipole vector is  $\mathbf{p}_\infty = (0, 0)^T$ . The spatially uniform theoretical prediction for the outer solution is  $P \sim v_\infty^* + o(\varepsilon)$  where  $v_\infty^* \approx 8.745 \times 10^{-4}$ . Left panel: Contour plot of  $P$  from FlexPDE at  $\varepsilon = 0.05$  showing no dipole effect.

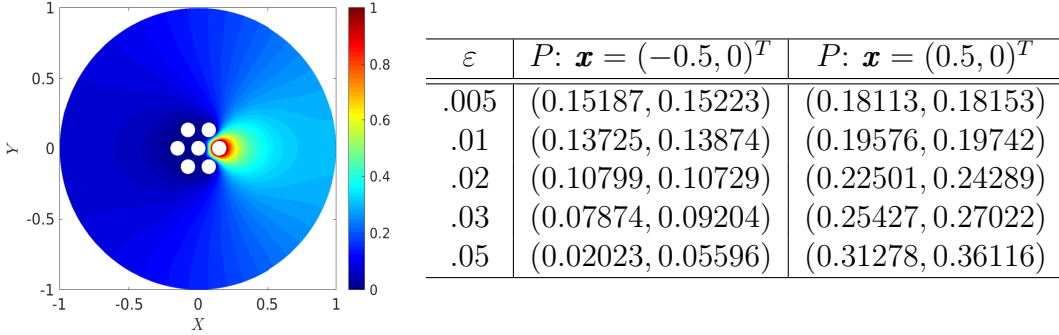


Figure 12: Right panel: The two-term asymptotic result  $P_a$  in (3.12) with  $v_\infty^* \approx 0.1665$  and dipole vector  $\mathbf{p}_\infty \approx (1.1702, 0)^T$  is compared at  $\mathbf{x} = (\pm 0.5, 0)^T$  with the FlexPDE numerical result  $P_n$  in the form  $(P_a, P_n)$  for a hexagonal trap cluster centered at the origin of the unit disk with  $l_c = 3$ . The target trap with  $P = 1$  is at the rightmost edge of the cluster. Left panel: Contour plot of  $P$  from FlexPDE at  $\varepsilon = 0.05$  showing the dipole.

## 4 Spatially periodic trap patterns

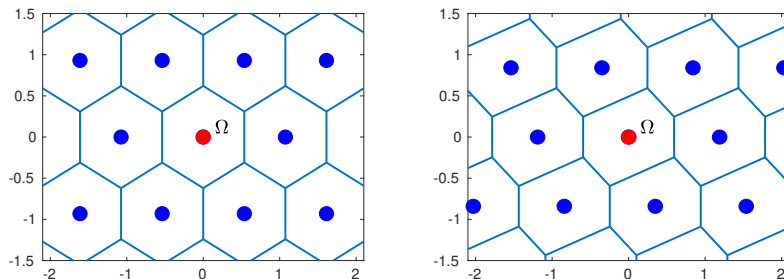


Figure 13: Left panel: Wigner Seitz (WS), or Voronoi, cells for a hexagonal pattern of circular traps (blue dots) of a common radius  $\varepsilon$ . The fundamental WS cell  $\Omega$  of unit area is centered at the origin and contains the red trap. The lattice vectors are  $\mathbf{l}_1 = \left( \left(\frac{4}{3}\right)^{1/4}, 0 \right)^T$  and  $\mathbf{l}_2 = \left(\frac{4}{3}\right)^{1/4} \left(\frac{1}{2}, \frac{\sqrt{3}}{2}\right)^T$ . Right panel: an oblique lattice with unit area of the primitive cell with generators  $\mathbf{l}_1 = \left(2^{1/4}, 0\right)^T$  and  $\mathbf{l}_2 = 2^{-1/4} (1, 1)^T$ .

In this section we consider a spatially periodic array of traps in  $\mathbb{R}^2$  where either a single trap or a trap cluster of small  $\mathcal{O}(\varepsilon)$  measure is centered at the lattice points of an oblique Bravais lattice  $\Lambda$  defined by

$$\Lambda \equiv \left\{ m\mathbf{l}_1 + n\mathbf{l}_2 \mid m, n \in \mathbb{Z} \right\}, \quad (4.1)$$

where  $\mathbb{Z}$  denotes the set of integers. We recall that the *Wigner-Seitz (WS)* cell centered at a fixed  $\mathbf{l} \in \Lambda$  is the set of all points in the plane that are closer to  $\mathbf{l}$  than to any other lattice point. The fundamental WS cell  $\Omega$  is the one centered at the origin (see Fig. 13 with the red trap). A WS cell is a convex polygon that has the same area  $|\mathbf{l}_1 \times \mathbf{l}_2|$  of the primitive cell, and the union of these WS cells tile all of  $\mathbb{R}^2$ . We will choose the lengthscale so that the area of the primitive cell is fixed at unity. For a hexagonal and a particular oblique lattice, in Fig. 13 we show the WS cells with a single circular trap (blue disk) of radius  $\varepsilon$  centered at each lattice point, and the fundamental WS cell  $\Omega$  centered at the origin (red disk).

### 4.1 The MFPT

The determination of the MFPT for the spatially periodic pattern of localized traps in  $\mathbb{R}^2$  can be reduced to a problem defined on the fundamental WS cell

$\Omega$ , which is formulated as

$$\Delta T = -\frac{1}{D}, \quad \mathbf{x} \in \Omega \setminus \Omega_\varepsilon; \quad T \in \mathcal{P}, \quad \mathbf{x} \in \partial\Omega, \quad (4.2a)$$

$$T = 0, \quad \mathbf{x} \in \partial\Omega_\varepsilon. \quad (4.2b)$$

Here  $\Omega_\varepsilon$  denotes a possibly multiply connected trap cluster of measure  $\mathcal{O}(\varepsilon)$  centered at the origin  $\mathbf{0} \in \Omega$ , while the set  $\mathcal{P}$  denotes periodic boundary conditions on  $\partial\Omega$  (see equation (2.35) of [9] for a precise description of  $\mathcal{P}$ ). In the limit  $\varepsilon \rightarrow 0$ , we will calculate the average MFPT

$$\bar{T} \equiv \frac{1}{|\Omega \setminus \Omega_\varepsilon|} \int_{\Omega \setminus \Omega_\varepsilon} T \, d\mathbf{x}, \quad \text{with } |\Omega \setminus \Omega_\varepsilon| = 1 - |\Omega_\varepsilon|, \quad (4.3)$$

where  $|\Omega_\varepsilon|$  is the area of the trap cluster.

The asymptotic analysis of (4.2) as  $\varepsilon \rightarrow 0$  relies on the periodic source-neutral Green's function  $G_p(\mathbf{x})$  with regular part  $R_p$ , defined uniquely by

$$\Delta G_p = \frac{1}{|\Omega|} - \delta(\mathbf{x}), \quad \mathbf{x} \in \Omega; \quad G_p \in \mathcal{P}, \quad \mathbf{x} \in \partial\Omega; \quad \int_{\Omega} G_p \, d\mathbf{x} = 0, \quad (4.4a)$$

$$G_p \sim -\frac{1}{2\pi} \log |\mathbf{x}| + R_p + \frac{|\mathbf{x}|^2}{4} + o(|\mathbf{x}|^2), \quad \text{as } \mathbf{x} \rightarrow \mathbf{0}. \quad (4.4b)$$

We remark that since  $\Omega$  has two lines of symmetry that intersect at the origin, the usual gradient term  $\nabla_{\mathbf{x}} G_p|_{\mathbf{x}=\mathbf{0}} \cdot \mathbf{x}$  is absent in the local behavior (4.4b).

In [4] an explicit formula for  $G_p(\mathbf{x})$  and  $R_p$  was derived in their analysis of droplet patterns in diblock copolymer theory. By identifying a point  $\mathbf{x}$  as a complex number  $z = x + iy$  and by writing the Bravais lattice equivalently in terms of generators  $\alpha \in \mathbb{C}$  and  $\beta \in \mathbb{C}$  as  $\Lambda \equiv \left\{ m\alpha + n\beta \mid m, n \in \mathbb{Z} \right\}$ , with  $\text{Im}(\beta/\alpha) > 0$  and  $\text{Im}(\bar{\alpha}\beta) = 1$  to fix the area of the primitive cell to unity, it was derived in [4] that

$$\begin{aligned} G_p = & \text{Im} \left( \frac{|z|^2 - \bar{\alpha}z^2/\alpha}{2(\alpha\bar{\beta} - \bar{\alpha}\beta)} - \frac{z}{2\alpha} + \frac{\beta}{12\alpha} \right) \\ & - \frac{1}{2\pi} \log \left| \left( 1 - e\left(\frac{z}{\alpha}\right) \right) \times \prod_{n=1}^{\infty} \left( 1 - e\left(\frac{n\beta + z}{\alpha}\right) \right) \left( 1 - e\left(\frac{n\beta - z}{\alpha}\right) \right) \right|, \end{aligned} \quad (4.5)$$

where  $e(w)$  is defined by  $e(w) \equiv e^{2\pi iw}$  and where the overbar denotes complex conjugate. Upon defining  $\zeta \equiv \beta/\alpha$  the regular part  $R_p$  of  $G_p$  is

$$R_p = -\frac{1}{2\pi} \log(2\pi) - \frac{1}{2\pi} \log \left| \sqrt{\text{Im}(\zeta)} e\left(\frac{\zeta}{12}\right) \prod_{n=1}^{\infty} (1 - e(n\zeta))^2 \right|. \quad (4.6)$$

In terms of  $R_p$  our asymptotic result for the average MFPT is as follows:

**Principal Result 4.1:** *For  $\varepsilon \rightarrow 0$ , the average MFPT (4.3) for (4.2) for an arbitrary oblique Bravais lattice is*

$$\bar{T} \sim \frac{1}{2\pi D} (-\log[\varepsilon d_c]) + \frac{R_p}{D} + o(1), \quad \text{as } \varepsilon \rightarrow 0, \quad (4.7)$$

where  $R_p$  is given in (4.6). Here  $d_c$  is the logarithmic capacitance of the re-scaled trap cluster  $\Omega_0 \equiv \varepsilon^{-1}\Omega_\varepsilon$ , as defined by the local problem

$$\begin{aligned} \Delta_{\mathbf{y}} v_c &= 0, \quad \mathbf{y} \notin \Omega_0; \quad v_c = 0, \quad \mathbf{y} \in \partial\Omega_0, \\ v_c &\sim \log |\mathbf{y}| - \log d_c + o(1), \quad \text{as } |\mathbf{y}| \rightarrow \infty. \end{aligned} \quad (4.8)$$

For the special case where  $\Omega_\varepsilon$  is a disk of radius  $\varepsilon$  we have the refined estimate

$$\bar{T} \sim \frac{1}{2\pi D} (-\log \varepsilon) + \frac{R_p}{D} + \frac{\varepsilon^2}{D} \left[ -\frac{1}{2} \log \varepsilon + \pi R_p + \frac{1}{2} \right] + o(\varepsilon^2), \quad \text{as } \varepsilon \rightarrow 0. \quad (4.9)$$

To establish these results for (4.2) we use strong localized perturbation theory as in [20]. In the inner region near  $\Omega_\varepsilon$  we introduce the inner variables

$$\mathbf{y} = \varepsilon^{-1}\mathbf{x}, \quad v(\mathbf{y}) \equiv T(\varepsilon\mathbf{y}), \quad (4.10)$$

and we expand the inner solution as

$$v(\mathbf{y}) = Av_c(\mathbf{y}) + \mu(\varepsilon)v_1(\mathbf{y}) + \dots, \quad (4.11)$$

where  $A = A(\nu)$ , with  $\nu \equiv -1/\log(\varepsilon d_c)$ , is to be found and  $\mu \ll \nu^k$  for any  $k > 0$ . Here  $v_c(\mathbf{y})$  is the solution to the local problem (4.8) that defines the logarithmic capacitance  $d_c$  of the trap cluster.

The dominant far-field behavior for the inner expansion (4.11) provides the asymptotic matching condition  $T \sim A \log |\mathbf{x}| + A/\nu + o(1)$  as  $\mathbf{x} \rightarrow 0$ . As such, in order to account for all terms in powers of  $\nu$ , we pose the outer expansion as

$$T \sim T_0(\mathbf{x}; \nu) + \sigma(\varepsilon)T_1 + \dots, \quad (4.12)$$

where the transcendentally small correction term  $\sigma(\varepsilon)$ , with  $\sigma(\varepsilon) \ll \nu^k$  for any  $k > 0$ , is determined below. We obtain that  $T_0$  satisfies

$$\begin{aligned} \Delta T_0 &= -\frac{1}{D}, \quad \mathbf{x} \in \Omega \setminus \{\mathbf{0}\}; \quad T_0 \in \mathcal{P}, \quad \mathbf{x} \in \partial\Omega, \\ T_0 &\sim A \log |\mathbf{x}| + \frac{A}{\nu}, \quad \text{as } \mathbf{x} \rightarrow 0. \end{aligned} \quad (4.13)$$

Since  $|\Omega| = 1$ , by the divergence theorem we calculate  $A = 1/(2\pi D)$  and we identify that

$$T_0 = \frac{1}{D} (-G_p(\mathbf{x}) + \chi_0), \quad (4.14)$$

where  $\chi_0$  is an undetermined constant. Finally, by matching (4.14) to the regular part of the singularity condition in (4.13) as  $\mathbf{x} \rightarrow \mathbf{0}$ , we obtain  $\chi_0 = R_p + 1/(2\pi\nu)$ . Then, upon integrating (4.14) over  $\Omega \setminus \Omega_\varepsilon$ , we obtain (4.7).

Next, we will calculate the first transcendently small term of order  $\mathcal{O}(\varepsilon^2)$  for the special case when  $\Omega_\varepsilon$  is a disk of radius  $\varepsilon$  for which  $d_c = 1$ . By writing the local behavior for  $G_p$  in (4.4b) in terms of the inner variable  $\mathbf{y}$  we obtain from (4.14) and (4.12) that

$$T \sim \frac{1}{2\pi D} \log |\mathbf{y}| - \frac{\varepsilon^2}{4D} |\mathbf{y}|^2 + \sigma(\varepsilon)T_1 + \dots, \quad (4.15)$$

with the  $\mathcal{O}(\varepsilon^2)$  term providing the scale of the correction term in the inner region. Therefore, we must choose  $\mu(\varepsilon) = \varepsilon^2$  in the inner expansion (4.11). For the disk-shaped trap we have  $v_c = \log |\mathbf{y}|$  and that  $v_1$  in (4.11) satisfies

$$\Delta_{\mathbf{y}} v_1 = -\frac{1}{D}, \quad |\mathbf{y}| \geq 1; \quad v_1 = 0 \text{ on } |\mathbf{y}| = 1; \quad v_1 \sim -\frac{|\mathbf{y}|^2}{4D} \text{ as } |\mathbf{y}| \rightarrow \infty, \quad (4.16)$$

which has the exact solution  $v_1 = (1 - |\mathbf{y}|^2)/(4D)$ . By matching  $v_1$  to the outer expansion (4.12) we conclude that  $\sigma(\varepsilon) = \varepsilon^2$  and that  $T_1$  satisfies

$$\Delta T_1 = 0, \quad \mathbf{x} \in \Omega \setminus \{\mathbf{0}\}; \quad T_1 \in \mathcal{P}, \quad \mathbf{x} \in \partial\Omega; \quad T_1 \rightarrow \frac{1}{4D}, \quad \text{as } \mathbf{x} \rightarrow \mathbf{0}, \quad (4.17)$$

which has the trivial solution  $T_1 = 1/(4D)$ . In this way, for a circular trap, we obtain the refined outer and inner solutions

$$T \sim \frac{1}{D} \left[ \frac{-\log \varepsilon}{2\pi} - G_p(\mathbf{x}) + R_p \right] + \frac{\varepsilon^2}{4D} + \dots, \quad \text{for } |\mathbf{x}| \gg \mathcal{O}(\varepsilon), \quad (4.18a)$$

$$v \sim \frac{1}{2\pi D} \log |\mathbf{y}| + \frac{\varepsilon^2}{4D} (1 - |\mathbf{y}|^2) + \dots, \quad \text{for } |\mathbf{y}| = \frac{|\mathbf{x}|}{\varepsilon} = \mathcal{O}(1). \quad (4.18b)$$

By using the local behavior for  $G_p(\mathbf{x})$  in (4.4b) we readily observe that the outer expansion (4.18a) contains the inner expansion (4.18b). As such, in estimating  $\bar{T}$  in (4.3) we need only integrate the outer expansion (4.18a) as

$$\bar{T} \sim \frac{1}{D(1 - \pi\varepsilon^2)} \int_{\Omega \setminus \Omega_\varepsilon} \left( R_p - \frac{\log \varepsilon}{2\pi} + \frac{\varepsilon^2}{4} \right) d\mathbf{x} - \frac{1}{D(1 - \pi\varepsilon^2)} \int_{\Omega \setminus \Omega_\varepsilon} G_p d\mathbf{x}, \quad (4.19a)$$

$$\sim \frac{1}{D} \left( R_p + \frac{(-\log \varepsilon)}{2\pi} + \frac{\varepsilon^2}{4} \right) + \frac{1}{D(1 - \pi\varepsilon^2)} \int_{\Omega_\varepsilon} G_p d\mathbf{x}, \quad (4.19b)$$

where we used  $\int_{\Omega \setminus \Omega_\varepsilon} G_p d\mathbf{x} = -\int_{\Omega_\varepsilon} G_p d\mathbf{x}$  since  $\int_{\Omega} G_p d\mathbf{x} = 0$ . Then, by using the local behavior in (4.4b), we get  $\int_{\Omega_\varepsilon} G_p d\mathbf{x} \sim -\frac{\varepsilon^2}{2} \log \varepsilon + \varepsilon^2/4 + \pi\varepsilon^2 R_p$ . By using this estimate in (4.19b), we obtain (4.9) from an explicit integration. This completes the derivation of Principal Result 4.1.

We remark that it is an open problem to determine the leading transcendently small term for the average MFPT for a trap cluster at the origin. However, for the MFPT (and not its spatial average), the dipole term  $\mathbf{p}_c$  in the far-field expansion in (2.4) determines the correction term to the MFPT in the outer region. More specifically, we have in the outer region that  $T \sim T_0 + \varepsilon T_1$ , where  $T_1$  satisfies  $\Delta T_1 = D^{-1} \mathbf{p}_c \cdot \nabla_{\mathbf{x}} \delta(\mathbf{x})$  with  $T_1 \in \mathcal{P}$  on  $\partial\Omega$ .

For a Bravais lattice with unit area of the primitive cell, it was proved in Theorem 2 of [4] that the regular part  $R_p$  in (4.6) is minimized for a regular hexagonal lattice. From Principal Result 4.1, this establishes that, over this class of lattices, the average MFPT is smallest for the hexagonal lattice.

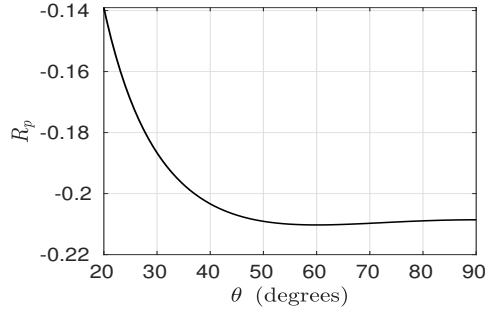


Figure 14: Plot of the regular part  $R_p$ , as given in (4.20), for the periodic source-neutral Green's function for oblique lattices with unit area of the primitive cell for which  $\mathbf{l}_1 = (1/\sqrt{\sin(\theta)}, 0)^T$  and  $\mathbf{l}_2 = (\cos(\theta)/\sqrt{\sin(\theta)}, \sqrt{\sin(\theta)})^T$ . The minimum occurs for the hexagon for which  $\theta = 60^\circ$ .

Next, we illustrate (4.6) for the one-parameter family of lattices  $\Lambda$  given by  $\mathbf{l}_1 = (1/\sqrt{\sin(\theta)}, 0)^T$  and  $\mathbf{l}_2 = (\cos(\theta)/\sqrt{\sin(\theta)}, \sqrt{\sin(\theta)})^T$ , for which  $|\mathbf{l}_1| = |\mathbf{l}_2|$ . This corresponds to setting  $\alpha = 1/\sqrt{\sin \theta}$  and  $\beta = \alpha e^{i\theta}$  in (4.6), which yields

$$R_{p0} = -\frac{1}{2\pi} \ln(2\pi) - \frac{1}{2\pi} \ln \left| \sqrt{\sin \theta} e^{\pi i \xi / 6} \prod_{n=1}^{\infty} (1 - e^{2\pi i n \xi})^2 \right|, \quad \xi = e^{i\theta}. \quad (4.20)$$

In Fig. 14 we plot  $R_{p0}$  versus  $\theta$  for this class of lattices. For the hexagonal lattice, where  $\theta = \pi/3$ , we calculate  $R_{p0} \approx -0.210262$ , while for the square

lattice, where  $\theta = \pi/2$ , we have  $R_{p0} \approx -0.208578$ . From the leading-order result (4.7), we have

$$\begin{aligned}\bar{T} &\sim \frac{1}{2\pi D} [-\log(\varepsilon d_c) - 1.310533 + o(1)] , \quad (\text{square}) \\ \bar{T} &\sim \frac{1}{2\pi D} [-\log(\varepsilon d_c) - 1.321117 + o(1)] , \quad (\text{hexagon}).\end{aligned}\tag{4.21}$$

Here  $d_c$  is the logarithmic capacitance of the trap cluster, as defined by the local problem (4.8).

For a circular trap of radius  $\varepsilon$ , for which  $d_c = 1$ , the leading-order result (4.21) for the square lattice was derived previously in equation (36) of [16] by using the method of pseudo-potentials and from the numerical evaluation of a certain discrete lattice sum. However, in [16] no estimate of the next term in the expansion of  $\bar{T}$  was provided. This estimate is provided by the more refined result (4.9), which yields

$$\begin{aligned}\bar{T} &\sim \frac{1}{2\pi D} (-\log \varepsilon - 1.310533) + \frac{\varepsilon^2}{D} \left( -\frac{1}{2} \log \varepsilon - 0.155266 \right) , \quad (\text{square}) \\ \bar{T} &\sim \frac{1}{2\pi D} (-\log \varepsilon - 1.321117) + \frac{\varepsilon^2}{D} \left( -\frac{1}{2} \log \varepsilon - 0.160559 \right) , \quad (\text{hexagon}).\end{aligned}\tag{4.22}$$

## 5 Discussion

The asymptotic calculation of the MFPT and the splitting probability in 2-D domains with small traps of radius  $\mathcal{O}(\varepsilon)$  has previously been restricted to the case where the traps are isolated in the sense that their center-to-center separation is  $\mathcal{O}(1)$  as  $\varepsilon \rightarrow 0$  (cf. [11], [5]). By adapting the simple series-based numerical approach of [17], we have shown how to readily incorporate the effect of a cluster of closely spaced circular traps into the asymptotic framework of [11] and [5] for the MFPT and splitting probability. For a target trap located within a cluster of traps, we have shown that we need to extend the asymptotic theory of [11] to one higher order so as to include the effect of the dipole vector for the trap cluster, which provides positional information about the target trap within the cluster. For a general trap cluster, this dipole vector is calculated numerically from extending the least-squares fitting procedure of [17]. An exact solution for the dipole vector for a two-trap cluster provides partial confirmation of the numerical result. Results from the extended asymptotic theory for the splitting probability were favorably compared with full FlexPDE numerical simulations for a few examples with trap clusters, which have clear qualitative interpretations.

We have also provided asymptotic expansions for the average MFPT for a cluster of traps centered at the lattice points of an arbitrary Bravais lattice in  $\mathbb{R}^2$ . Our analysis for this problem has relied on an explicit formula for the regular part of the periodic source-neutral Green's function, as derived in [4], within the fundamental Wigner-Seitz cell of the lattice. For the special case of a circular trap and for a square lattice our asymptotic result agrees with that in [16], and provides the dominant transcendently small terms in the expansion not provided in [16].

**Acknowledgements** M. J. Ward gratefully acknowledges the financial support of the NSERC Discovery Grant Program (Canada).

## A Dipole Moment: Two-Trap Cluster

In this appendix we derive a formula for the dipole vector  $\mathbf{p}_\infty$  from the solution to (2.4) for a two-trap cluster where the two traps are

$$\Omega_{1,1} = \{\mathbf{y} \mid |\mathbf{y} - (l_c/2, 0)^T| \leq 1\}, \quad \Omega_{1,2} = \{\mathbf{y} \mid |\mathbf{y} + (l_c/2, 0)^T| \leq 1\}, \quad (\text{A.1})$$

where  $l_c > 2$ . To solve (2.4) for the two-trap cluster (A.1) we follow Appendix A of [11] and introduce bipolar coordinates  $\xi$  and  $\eta$ , as defined by

$$y_1 = \frac{c \sinh \xi}{\cosh \xi - \cos \eta}, \quad y_2 = \frac{c \sin \eta}{\cosh \xi - \cos \eta}, \quad \text{with } c = \sqrt{\frac{l_c^2}{4} - 1}. \quad (\text{A.2})$$

Then,  $|\mathbf{y}| \rightarrow \infty$  corresponds to  $(\xi^2 + \eta^2)^{1/2} \rightarrow 0$ , and the two disks are mapped to the coordinate lines  $\xi = \pm \xi_1$  where  $\xi_1 \equiv \cosh^{-1}(l_c/2)$ .

By introducing these bipolar coordinates in (2.4), we readily derive that  $V^*(\xi, \eta) \equiv v^*[y_1(\xi, \eta), y_2(\xi, \eta)]$  satisfies

$$\begin{aligned} V_{\xi\xi}^* + V_{\eta\eta}^* &= 0, \quad |\xi| \leq \xi_1, \quad |\eta| \leq \pi, \\ V^* &= 0 \quad \text{on } \xi = -\xi_1; \quad V^* = 1 \quad \text{on } \xi = \xi_1, \\ V^*, V_\eta^* & \quad 2\pi \text{ periodic in } \eta, \end{aligned} \quad (\text{A.3})$$

which has the exact solution

$$V^* = \frac{1}{2} + \frac{\xi}{2\xi_1}, \quad \text{where } \xi_1 \equiv \cosh^{-1}(l_c/2). \quad (\text{A.4})$$

Finally, we let  $|\mathbf{y}| \rightarrow \infty$  in the mapping (A.2) which corresponds to  $\xi^2 + \eta^2 \rightarrow 0$ . From a Taylor expansion of (A.2), we derive that

$$y_1 \sim \frac{2c\xi}{\xi^2 + \eta^2}, \quad y_2 \sim \frac{2c\eta}{\xi^2 + \eta^2}, \quad (\text{A.5})$$

which yields  $\xi^2 + \eta^2 \sim 4c^2/(y_1^2 + y_2^2)$ . This shows that  $\xi \sim 2cy_1/(y_1^2 + y_2^2)$  as  $|\mathbf{y}| \rightarrow \infty$ . Upon substituting this expression into (A.4) we obtain the following far-field behavior for the solution to (2.4):

$$v^* \sim \frac{1}{2} + \frac{c}{\xi_1} \frac{y_1}{y_1^2 + y_2^2}, \quad \text{as } |\mathbf{y}| \rightarrow \infty. \quad (\text{A.6})$$

By recalling (A.2) and (A.4) for  $c$  and  $\xi_1$ , respectively, we obtain (3.11) for the dipole vector  $\mathbf{p}_\infty$ .

## References

- [1] O. Bénichou and R. Voituriez. “From first-passage times of random walks in confinement to geometry-controlled kinetics”. In: *Physics Reports* 539.4 (2014), pp. 225–284 (cit. on p. 2).
- [2] P. C. Bressloff. *Asymptotic analysis of extended two-dimensional narrow capture problems*. submitted to Proc. Roy. Soc. A. 2020 (cit. on p. 2).
- [3] P. C. Bressloff. “Search processes with stochastic resetting and multiple targets”. In: *Phys. Rev. E*. 102 (2020), p. 022115 (cit. on p. 2).
- [4] X. Chen and Y. Oshita. “An application of the modular function in nonlocal variational problems”. In: *Arch. Rat. Mech. Anal.* 186.1 (2007), pp. 109–132 (cit. on pp. 4, 19, 22, 24).
- [5] D. Coombs, R. Straube, and M. Ward. “Diffusion on a sphere with localized traps: Mean first passage time, eigenvalue asymptotics, and Fekete points”. In: *SIAM J. Appl. Math.* 70.1 (2009) (cit. on pp. 2, 23).
- [6] FlexPDE. *PDE Solutions inc*. Available at <http://www.pdesolutions.com>. 2015 (cit. on pp. 3, 9, 14, 15, 17).
- [7] D. Holcman and Z. Schuss. “The Narrow Escape Problem”. In: *SIAM Review* 56.2 (2014), pp. 213–257 (cit. on p. 2).
- [8] D. Holcman and Z. Schuss. “Time scale of diffusion in molecular and cellular biology”. In: *J. of Physics A: Math. and Theor.* 47.17 (2014), p. 173001 (cit. on p. 2).
- [9] D. Iron et al. “Logarithmic expansions and the stability of periodic patterns of localized spots for reaction-diffusion systems in  $\mathbb{R}^2$ ”. In: *J. Nonlin. Science* 24.5 (2014), pp. 564–627 (cit. on p. 19).

- [10] T. Kolokolnikov, M. S Titcombe, and M. J Ward. “Optimizing the fundamental Neumann eigenvalue for the Laplacian in a domain with small traps”. In: *European Journal of Applied Mathematics* 16.2 (2005), pp. 161–200 (cit. on p. 7).
- [11] V. Kurella et al. “Asymptotic analysis of first passage time problems inspired by ecology”. In: *Bulletin of Mathematical Biology* 77.1 (2015) (cit. on pp. 2–4, 6, 10, 13, 23, 24).
- [12] A. E. Lindsay, J. C. Tzou, and T. Kolokolnikov. “Narrow escape problem with mixed trap and the effect of orientation”. In: *Phys. Rev. E* 91.3 (2015), p. 032111 (cit. on p. 2).
- [13] T. Ransford. *Potential theory in the complex plane*. London Math. Soc. Stud. Texts 28. Cambridge, U.K.: Cambridge University Press, 1995 (cit. on p. 3).
- [14] S. Redner. *A guide to first-passage processes*. Cambridge University Press, 2001 (cit. on pp. 4, 10).
- [15] A. Singer, Z. Schuss, and D. Holcman. “Narrow escape, Part II: The circular disk”. In: *J. Stat. Phys.* 122.3 (2006), pp. 465–489 (cit. on p. 2).
- [16] D. C. Torney and B. Goldstein. “Rates of diffusion-limited reaction in periodic systems”. In: *J. Stat. Phys.* 49 (1987), pp. 725–750 (cit. on pp. 4, 23, 24).
- [17] N. Trefethon. “Series solution of Laplace Problems”. In: *ANZIAM J.* 60 (2018), pp. 1–26 (cit. on pp. 1–3, 6, 11, 23).
- [18] M. J Ward. “Spots, traps, and patches: Asymptotic analysis of localized solutions to some linear and nonlinear diffusive systems”. In: *Nonlinearity* 31.8 (2018), R189 (cit. on pp. 2, 4).
- [19] M. J. Ward, W. D. Henshaw, and J. B. Keller. “Summing logarithmic expansions for singularly perturbed eigenvalue problems”. In: *SIAM J. Appl. Math.* 53.3 (1993), pp. 799–828 (cit. on pp. 2, 4).
- [20] M. J Ward and J. B Keller. “Strong localized perturbations of eigenvalue problems”. In: *SIAM Journal on Applied Mathematics* 53.3 (1993), pp. 770–798 (cit. on pp. 2, 20).

## Author addresses

1. **S. Iyaniwura**, Department of Mathematics, University of British Columbia, Vancouver, British Columbia, CANADA.  
<http://www.math.ubc.ca>

2. **M. J. Ward**, Department of Mathematics, University of British Columbia, Vancouver, British Columbia, CANADA.  
mailto:ward@math.ubc.ca  
orcid:0000-0001-6959-7202